

# Microcontact Printing of Lipophilic Self-Assembled Monolayers for the Attachment of Biomimetic Lipid Bilayers to Surfaces

A. Toby A. Jenkins,<sup>†</sup> Neville Boden,<sup>†</sup> Richard. J. Bushby,<sup>†</sup> Stephen. D. Evans,<sup>\*,†</sup> Peter. F. Knowles,<sup>†</sup> Robert. E. Miles,<sup>†</sup> Simon. D. Ogier,<sup>†</sup> Holger Schönherr,<sup>‡</sup> and G. Julius Vancso<sup>‡</sup>

Contribution from the Centre for Self-Organising Molecular Systems, University of Leeds, Leeds LS2 9JT, U.K., and Faculty of Chemical Technology, Polymer Materials Science and Technology, University of Twente, P.O. Box 217, NL-7500 AE Enschede, The Netherlands

Received November 17, 1998

**Abstract:** This paper presents a novel method for supporting planar lipid bilayers using microcontact printed lipophilic self-assembled monolayers, in such a way as to retain their capacity to support biological functionality. Impedance spectroscopy, surface plasmon resonance, and atomic force microscopy are used to monitor the formation and investigate the properties of the supported bilayers. In addition, we show that the antibiotic peptide gramicidin and the ionophore valinomycin exhibit the expected ion selectivity. Finally, scanning force microscopy measurements show surface friction changes following bilayer formation. Chemically modified tips were used to obtain information about both the energy of the surface (hydrophobic/hydrophilic nature) and the mechanical properties of the surface.

## Introduction

The cytoplasmic membrane is a lipid bilayer that serves to separate the environment inside a cell from that outside. Such membrane structures while fluid have long-term stability and are effective barriers against the transport of water soluble ions and molecules. Generally, such membranes have proteins (as well as carbohydrates and sugars) associated with them which may be integral (within the membrane) or peripheral (at the membrane surface). These proteins are involved in a wide range of cellular activity, for example, in the mediated permeation of metabolites, signal transduction, and immunoresponse. Many of the mechanisms underlying these processes rely on the *high specificity* of ligand–protein binding events, and this has prompted great interest in their use for the development of biosensors. There are a variety of approaches one could take to make use of the high specificity of such protein binding systems, for example, one might isolate the receptor responsible for the ligand binding and use spectroscopic techniques to follow binding events. Such an approach is only feasible if the receptor is stable and maintains its function outside of its membrane environment. Alternatively, one could follow a “biomimetic” approach whereby a protein is placed in a phospholipid membrane, or a natural membrane fragment, attached to a solid support. This latter approach is currently under investigation by a number of research groups and is attractive in that it allows interrogation via potentiometric/impedance techniques (for systems in which ligand binding changes the permeability of the membrane to ions and for which there is an ion gradient across the membrane).

The most straightforward approach has been to attach a lipid film to a surface, adsorbed either directly on the substrate or onto a self-assembled monolayer (SAM) modified surface. For

example, lipid monolayers containing the antibiotic gramicidin have been adsorbed onto mercury drop electrodes and its channel forming properties investigated using  $\text{Ti}^+$  and  $\text{Ca}^{2+}$  electrochemistry.<sup>1</sup>

Plant et al. have examined adsorbed lipid monolayers on SAMs by using surface plasmon resonance (SPR), impedance spectroscopy, and vibrational spectroscopy.<sup>2–5</sup> The formation of lipid bilayers on SAMs containing defects showed that enzymes such as *E. coli* pyruvate oxidase could be incorporated into the lipid layer and retain enzymatic activity.<sup>6</sup> Similarly, the ganglioside  $\text{G}_{\text{M1}}$  that binds cholera toxin protein has been incorporated into adsorbed lipid monolayers on alkanethiol SAMs and the binding of the toxin investigated with SPR.<sup>7</sup> The formation of lipid bilayers directly adsorbed onto quartz substrates or phospholipid monolayer covered quartz has been investigated using total internal reflection fluorescence microscopy and found to have properties comparable to those formed by LB transfer.<sup>8</sup>

The Langmuir–Blodgett technique, in which molecules are transferred from the air–water interface to a solid substrate, has been exploited by a number of researchers as a method of attaching lipid membranes to surfaces.<sup>9,10</sup> The formation of patterned monolayers consisting of a thiol-lipid and palmitic

(1) Nelson, A. *Langmuir* **1996**, *12*, 2058–2067.

(2) Plant, A. L.; Brigham-Burke, M.; Petrella, E. C.; O'Shannessy, D. J. *Anal. Biochem.* **1995**, *226*, 342–348.

(3) Plant, A. L.; Gueguetchkeri, M.; Yap, W. *Biophys. J.* **1994**, *67*, 1126–1133.

(4) Plant, A. L. *Langmuir* **1993**, *9*, 2764–2767.

(5) Meuse, C. W.; Niaura, G.; Lewis, M. L.; Plant, A. L. *Langmuir* **1998**, *14*, 1604–1611.

(6) Pierrat, O.; Lechat, N.; Bourdillon, C.; Laval, J. M. *Langmuir* **1997**, *13*, 4112–4118.

(7) Terrettaz, S.; Stora, T.; Duschl, C.; Vogel, H. *Langmuir* **1993**, *9*, 1361–1369.

(8) Kalb, E.; Frey, S.; Tamm, L. K. *Biochim. Biophys. Acta* **1992**, *1103*, 307–316.

(9) Kühner, M.; Tampé, R.; Sackmann, E. *Biophys. J.* **1994**, *67*, 217–226.

<sup>†</sup> University of Leeds.

<sup>‡</sup> University of Twente.

\* To whom correspondence should be addressed. E-mail: s.d.evans@leeds.ac.uk.

acid at the air–water interface and subsequent transfer onto a solid substrate has been utilized by Duschl et al.<sup>11</sup> Following monolayer transfer, the palmitic acid was rinsed away, leaving a patterned thiol lipid attached to gold. Lipid adsorption onto such substrates allowed the formation of bilayer regions into which trans-membrane proteins could be incorporated.

The approach used in this paper is similar to that reported by Duschl et al., which used self-assembled monolayers of lipophilic molecules as a means of attaching lipid layers to surfaces.<sup>11,12</sup> Our approach differs in that the anchoring units used are lipophilic cholesterol molecules and that we form mixed SAMs. The second component of these “mixed” SAMs are short hydroxy-terminated thiols and are used to introduce a degree of disorder, while retaining a hydrophilic environment, beneath subsequently adsorbed lipid layers. The kinetics of lipid monolayer/bilayer formation on these SAMs and the structure of the adsorbed lipid layers have been studied using SPR and ATR–Fourier transform infrared (FTIR) spectroscopies, respectively.<sup>13–15</sup> Brink et al. have used a SAM consisting of cystamine to which they have covalently attached a derivatized lipid.<sup>16</sup> Raguse et al. have prepared lipid anchor molecules consisting of a poly(ethoxy acid) chain attached to a single lipid chain.<sup>17</sup> These lipid anchors were mixed with spacer molecules and allowed to self-assemble onto a gold substrate. Further lipid was then added to the mixed SAM to form a bilayer. Chemisorption of DMPE lipid onto self-assembled monolayers of thiol derivatized peptides has been achieved by activation of the COOH terminus of the peptide; this was followed by incorporation of ATPase protein into the DMPE bilayer.<sup>18</sup>

Polyelectrolytes on gold and silicon have been used to support bilayers and appear to meet the criteria of providing a flexible, aqueous environment for lipid bilayer assembly.<sup>18,19</sup>

The use of micropatterning to support lipid bilayers was first reported by Groves et al., who used grids of patterned, photoresist aluminium oxide and gold on silicon dioxide. Lipids were selectively adsorbed creating “corrals” of lipid bilayer confined by the patterned surface.<sup>20a,b</sup> It was also found that trans-membrane proteins were localized in the “corrals” (bilayer regions). More recently, Heyse et al. have used the selective photooxidation (by masking) of thiol derivatized surfaces to create patterned structures of anchoring units on gold surfaces.<sup>20c</sup>

We have previously demonstrated that microcontact printing, of a thiol ethoxy derivatized cholesterol molecule, can be used to form micropatterned surfaces suitable for anchoring phospholipid bilayers on gold substrates.<sup>21</sup> This use of microcontact

printing of SAMs to support lipid bilayers has several perceived benefits: First, the majority of the gold substrate is covered by an integral (blocking) SAM, thus reducing the leakage current of ions through areas of defective lipid layer.<sup>21</sup> Second, the spatial geometry (size and distribution of bilayers) can be controlled, allowing potential for optimization of the stamp geometry, e.g. the size, shape, and distribution of bilayer areas. Third, we expect incorporated transmembrane proteins to remain localized in bilayer regions in which they are adsorbed (i.e., to have a restriction of their lateral motion).<sup>20</sup>

A number of groups have started to use scanning force microscopy (SFM) to study patterned SAMs and lipid layers on surfaces. Differences in friction observed by SFM have been attributed to different chemical compositions of the surface, e.g. in phase-separated LB films<sup>22,23</sup> patterned SAMs,<sup>24</sup> or neat SAMs.<sup>25</sup> In friction measurements with chemically modified tips on patterned SAMs, the interaction between the functional groups exposed at the tip and the sample was shown to result in predictable frictional differences (“chemical force microscopy”).<sup>26,27</sup> The interpretation of the contrast is based on surface free energy arguments. Pull-off forces were shown to be directly correlated to the magnitude of the frictional force.<sup>28</sup> However, differences in friction were observed on surfaces with similar, or exactly the same, surface free energies. Apart from friction anisotropy on homogeneous samples, the dissipation of energy in self-assembled monolayers of thiols and silanes was found to influence their tribological properties significantly.<sup>29–34</sup> In addition, differences in contact area between the SFM tip and sample due to different packing densities in patterned SAMs or different mechanical properties of lipid bilayers were shown to result in variations of friction.<sup>35,36</sup>

In this paper, we demonstrate that micropatterning of thiol-terminated lipophilic SAMs can be used to support lipid membranes that meet the key criteria required for use as potential biosensors: (i) they are sufficiently ionically blocking for ion channel activity to be observed, (ii) they are formed over hydrophilic SAM regions (mercaptoethanol) and thus should have a water layer under the bilayer which is important for the addition of more complex ion channels especially for

(10) Stetzle, M.; Weissmüller, G.; Sackmann, E. *J. Phys. Chem.* **1993**, *97*, 2974–81.

(11) Duschl, C.; Liley, M.; Corradin, G.; Vogel, H. *Biophys. J.* **1994**, *67*, 1229–1237.

(12) Duschl, C.; Liley, M.; Lang, H.; Ghandi, A.; Zakeeruddin, S. M.; Stahlberg, H.; Dubochet, J.; Nemetz, A.; Knoll, W.; Vogel, H. *Mater. Sci. Eng. C* **1996**, *4*, 7–18.

(13) Williams, L. M.; Evans, S. D.; Flynn, T. M.; Marsh, A.; Knowles, P. F.; Bushby, R. J.; Boden, N. *Langmuir* **1997**, *13*, 751–757.

(14) Williams, L. M.; Evans, S. D.; Flynn, T. M.; Marsh, A.; Knowles, P. F.; Bushby, R. J.; Boden, N. *Supramol. Sci.* **1997**, *4*, 513–517.

(15) Cheng, Y.; Boden, N.; Bushby, R. J.; Clarkson, S.; Evans, S. D.; Knowles, P. F.; Marsh, A. *Langmuir* **1998**, *14*, 839–844.

(16) Brink, G.; Schmitt, L.; Tampé, R.; Sackmann, E. *Biochim. Biophys. Acta* **1994**, *1196*, 227–230.

(17) Raguse, B.; Braach-Maksvytis, V.; Cornell, B. A.; King, L. G.; Osman, P. D. J.; Pace, R. J.; Wiczorek, L. *Langmuir* **1998**, *14*, 648–659.

(18) Miller, L. S.; Rhoden, A. L.; Byrne, N.; Heptinstall, J.; Walton, D. J.; *Mater. Sci. Eng. C* **1995**, *3*, 187–90.

(19) Lindholm-Sethson, B. *Langmuir* **1996**, *12*, 3305–3314.

(20) (a) Groves, J. T.; Ulman, N.; Boxer, S. G. *Science* **1997**, *275*, 651–653. (b) Groves, J. T.; Wulfing, C.; Boxer, S. G. *Biophys. J.* **1996**, *71*, 2716–2723. (c) Heyse, S.; Ernst, O. P.; Dienes, Z.; Hofmann, K. P.; Vogel, H. *Biochemistry* **1998**, *37*, 507–522.

(21) Jenkins, A. T. A.; Bushby, R. J.; Boden, N.; Evans, S. D.; Knowles, P. F.; Miles, R. E.; Ogier, S. D. *Langmuir* **1998**, *14*, 4675–4678.

(22) Overney, R. M.; Meyer, E.; Frommer, J.; Brodbeck, D.; Lüthi, R.; Howald, L.; Güntherodt, H.-J.; Fujihira, M.; Takano, H.; Gotoh, Y. *Nature* **1992**, *359*, 133.

(23) Overney, R. M.; Meyer, E.; Frommer, J.; Güntherodt, H.-J.; Fujihira, M.; Takano, H.; Gotoh, Y. *Langmuir* **1994**, *10*, 1281.

(24) Wilbur, J. L.; Biebuyck, H. A.; MacDonald, J. C.; Whitesides, G. M. *Langmuir* **1995**, *11*, 825–831.

(25) Kim, H. I.; Koini, T.; Lee, T. R.; Perry, S. S. *Langmuir* **1997**, *13*, 7192.

(26) Frisbie, D.; Rozsnyai, L. F.; Noy, A.; Wrighton, M. S.; Lieber, C. M. *Science* **1994**, *265*, 2071.

(27) Noy, A.; Vezenov, D. V.; Lieber, C. M. *Annu. Rev. Mater. Sci.* **1997**, *27*, 381.

(28) Noy, A.; Frisbie, D.; Rozsnyai, L. F.; Wrighton, M. S.; Lieber, C. M. *J. Am. Chem. Soc.* **1995**, *117*, 7943.

(29) Mate, C. M.; McClelland, G. M.; Erlandsson, R.; Chiang, S. *Phys. Rev. Lett.* **1987**, *59*, 1942.

(30) Schönherr, H.; Vancso, G. J. *Macromolecules* **1997**, *30*, 6391 and references therein.

(31) Schönherr, H.; Kenis, P. J. A.; Harkema, S.; Hulst, R.; Engbersen, J. F. J.; Reinhoudt, D. N.; Vancso, G. J. *Langmuir* **1998**, submitted.

(32) Xiao, X.; Hu, J.; Charych, D. H.; Salmeron, M. *Langmuir* **1996**, *12*, 235.

(33) Lio, A.; Charych, D. H.; Salmeron, M. *J. Phys. Chem. B* **1997**, *101*, 3800–3805.

(34) Carpick, R. W.; Salmeron, M. *Chem. Rev.* **1997**, *97*, 1163–1194.

(35) Bar, G.; Rubin, S.; Parikh, A. N.; Swanson, B. I.; Zawodzinski, T. A., Jr.; Whangbo, M.-H. *Langmuir* **1997**, *13*, 373.

(36) Dufrène, Y. F.; Barger, W. R.; Green, J.-B. D.; Lee, G. U. *Langmuir* **1997**, *18*, 4779.

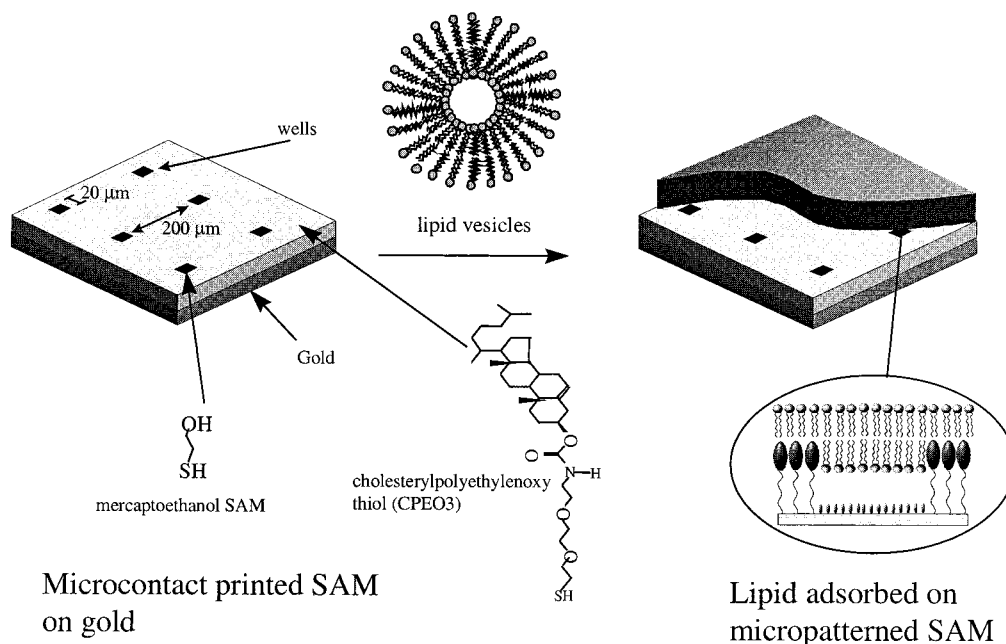


**Figure 1.** Schematic illustration of lipid bilayer formation on a micropatterned SAM.

proteins with large extramembraneous segments, and (iii) the bilayers appear to be relatively fluid (from comparing the frictional forces of the lipid-covered cholesterol and lipid-covered mercaptoethanol areas).

### Experimental Section

Gold electrodes for the electrochemical measurements were made by the thermal evaporation of 5 nm of chromium followed by 150 nm of gold onto cleaned glass microscope slides (2 min argon plasma) at a pressure of  $2 \times 10^{-6}$  mbar. Gold substrates for the SPR experiments were made by the thermal evaporation of 50 nm of gold onto a high refractive index glass prism. The construction of the microcontact printing stamps is detailed by Mrksich and Whitesides.<sup>37</sup> For the "masters", a negative photoresist, SU8, was spin-coated on glass then irradiated with UV light through a mask consisting of 200 μm lines, 20 μm apart. Following UV irradiation, the SU8 was developed to give a pattern of 20 μm parallel lines spaced by 200 μm. Poly(dimethyl siloxane) (PDMS) mixed with its cross-linking agent in a ratio of 10:1 was added onto the patterned SU8 and baked at 65 °C for 1 h. The "rubberized" PDMS was peeled from the photoresist to give a pattern of 200 μm lines, 20 μm lines apart.

This patterned elastomeric stamp was "inked" with CPEO3 molecules dissolved in dichloromethane (1 mM) and stamped on a "plasma-cleaned" gold electrode. The stamping procedure was performed twice on the same electrode; the second time the stamp was rotated 90° with respect to the first stamping of the electrode to form an array of 20 × 20 μm "wells" surrounded by CPEO3 molecules. The wells were "back-filled" with mercaptoethanol by placing the substrate in a 1 mM solution of mercaptoethanol in dichloromethane (Figure 1). An exception to this was on the micropatterned SAMs prepared for SFM measurements under fluid where it was difficult to locate the 20 × 20 μm "wells" due to their low density on the surface. For these experiments the surface was stamped once, so giving an series of parallel 20 μm wide lines filled with mercaptoethanol SAM, 200 μm apart.

**SAM Materials.** The preparation of the lipid "anchor" molecule, cholesteryl poly(ethyleneoxy) thiol (CPEO3) is detailed in ref 38. The "spacer" molecule, mercaptoethanol, was purchased commercially.

**Lipid Preparation.** Large unilamellar vesicles (LUVs) were formed from egg-phosphatidylcholine (EPC) (Lipid products, U.K.). EPC (5 mg) dissolved in chloroform/methanol was dried under a stream of

**Table 1.** Average Pull-Off Forces (nN) Measured in Millipore Water<sup>a</sup>

|                                    | silicon nitride tip on OH | silicon nitride tip on Chol | octadecane-thiol tip on OH | octadecane-thiol tip on Chol |
|------------------------------------|---------------------------|-----------------------------|----------------------------|------------------------------|
| prior to interaction with vesicles | 0.1                       | 0.3                         | 1.2                        | 13.0                         |
| after interaction with vesicles    | 3.0                       | 0.5                         | 0.2                        | 0.4                          |

<sup>a</sup> Data obtained from separate force measurements.

nitrogen and then hydrated in aqueous salt solution (0.1 M BaCl<sub>2</sub>). The dispersion was vortexed to ensure full dispersion of the lipid in the salt solution. The resultant dispersion was extruded 20 times through a membrane containing 100 nm diameter pores to form unilamellar vesicles of approximate diameter 90 nm.<sup>8</sup> These were then diluted to approximately 0.2 mg/mL.

**Scanning Force Microscopy.** The SFM images were obtained on a NanoScope III multimode scanning force microscope equipped with a liquid cell (Digital Instruments (DI), Santa Barbara, CA) filled with Millipore Milli-Q water. Standard silicon nitride tips on triangular-shaped cantilevers (DI) as well as chemically modified tips on cantilevers with a nominal cantilever spring constant of 0.06 N/m were used. Tips were modified by sputter-coating with ca. 50 nm of gold followed by deposition of a SAM of octadecanethiol from 1.0 mM solution in ethanol.<sup>30</sup> Monolayer-covered gold substrates (5 nm Ti, 200 nm Au evaporated in high vacuum onto borosilicate glass slides) were glued to the sample holder discs with cyan acrylate glue. Prior to imaging, the setup was equilibrated for at least 1 h. The imaging force<sup>39,40</sup> during the SFM experiments was minimized to ca. 1 nN. The sample was scanned at an angle of 90° with respect to the long axis of the cantilever, and the friction signals for both directions of the scan lines (trace and retrace) were captured simultaneously. (True differences in friction force can only be identified by a contrast reversal for trace (data collected while scanning from left to right) and retrace (right to left).) In addition, the pull-off forces between SFM tip and sample were measured and adhesion images were obtained.<sup>36,41</sup>

The adhesion images were obtained by collecting the force-distance plots laterally resolved for 64 × 64 pixels. The data are displayed in form of a layered image of the retracting part of the force-distance

(37) Mrksich, M.; Whitesides, G. M. *Trends Biotechnol.* **1995**, *13*, 228–235.

(38) Boden, N.; Bushby, R. J.; Clarkson, S.; Evans, S. D.; Knowles, P. F.; Marsh A. *Tetrahedron* **1997**, *53*, 10939–10952.

(39) Weisenhorn, A. L.; Hansma, P. K.; Albrecht, T. R.; Quate, C. F. *Appl. Phys. Lett.* **1989**, *54*, 2651.

(40) Weisenhorn, A. L.; Maivald, P.; Butt, H.-J.; Hansma, P. K. *Phys. Rev. B* **1992**, *45*, 11226.



curves, the so-called force volume images (DI). (The measured quantity is the pull-off force. We use "adhesion" as a synonym according to ref 41.)

**Electrochemical Impedance Measurements.** Electrochemical impedance measurements were made using a Solartron 1287 Electrochemical interface and 1260 impedance analyzer. A 10 mV amplitude AC potential was applied to a two-electrode electrochemical cell comprising of the membrane-covered working electrode and a gold foil counter electrode. The system was measured at its open circuit potential. The applied AC potential was scanned between 50 kHz and 300 mHz. Details of the fitting routine and the physical origin of the experimentally determined resistance and capacitance values are given elsewhere.<sup>21</sup> Measurements were carried out in different chloride salt solutions, depending on the desired cation. The cell was thoroughly flushed between different electrolytes, with Millipore water and four cell volumes of the desired electrolyte. All kinetics experiments were performed in 0.1 M BaCl<sub>2</sub>.

**Surface Plasmon Resonance Spectroscopy.** SPR measurements were made on a system built at the University of Leeds. A HeNe laser was directed onto a high refractive index glass (Halbo Optics, Chelmsford, U.K.) prism coated with 50 nm of gold. The ratio of the reflected to incident laser intensity was measured as a function of the angle of incidence to obtain a resonance spectrum. A Teflon flow cell was used to contain the aqueous ambient into which vesicle dispersions were added. Initially, the resonance curve of the microcontact printed SAM on gold was measured under 0.1 M KCl. From this curve an internal angle of  $\theta_{\min} - 0.5^\circ$  was defined for monitoring the kinetics of vesicle adsorption (intensity vs time, at a fixed angle of incidence). Two time regions were chosen: Initially, measurements were made every 0.5 s for the first 300 s to record the initial interaction of vesicles with the SAM. In the second regime, measurements were taken every 3 s for the remaining 6000 s of the experiment. Lipid vesicles were injected at a concentration of 0.5 mg/mL in 0.1 M NaCl (*vide supra*). Following the kinetics measurements, the cell was flushed thoroughly with 0.1 M NaCl and a second resonance curve obtained. This allows a quantification of the adsorbed lipid coverage.

## Results

**SFM Measurements.** The patterned samples were imaged before and after bilayer formation by SFM in different environments (air, liquids) and using different tip functionalities to determine the factors that are responsible for the observed contrast in friction mode. The bilayer formation was carried out in situ in the liquid cell of the SFM. (The in situ imaging of the bilayer formation was hampered by scattering of the SFM laser beam due to the vesicles.) Thus, SFM images were captured prior to and after bilayer formation. Prior to the addition of the vesicles a height difference of ca. 2 nm between the mercaptoethanol and the CPEO3 parts was observed (see the Supporting Information). After addition of lipid no height difference was observed. (The rms roughness of the gold was 3.6 nm, measured in images of  $1 \times 1 \mu\text{m}$ .)

**SFM in Air.** The patterned SAMs were investigated by SFM in air<sup>24</sup> prior to the interaction of the vesicles with the surface. The microcontact-printed pattern which exposes different functional groups was imaged in friction mode SFM (Figure 2). The friction force observed on the hydrophilic area of mercaptoethanol was significantly higher than the friction force on the hydrophobic areas composed of CPEO3 SAM. The same trend was observed in adhesion images. Capillary forces due to adsorbed water are likely to be responsible for the observed differences in friction and adhesion. On the hydrophilic mercaptoethanol parts, the water layer can be expected to be significantly thicker than on the hydrophobic cholesterol (cf. contact angles results).

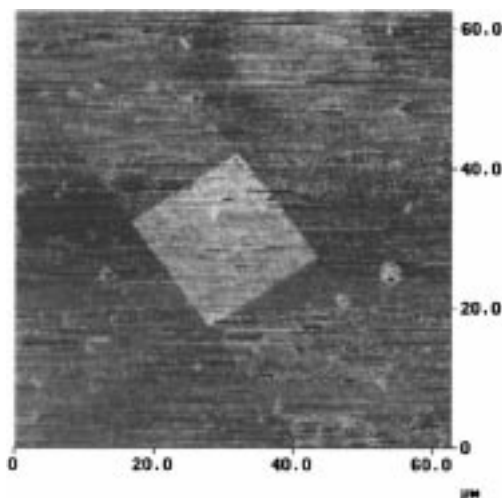


**Figure 2.** Friction force micrograph obtained with an unmodified SFM tip on a patterned SAM in air. Bright area denotes high friction ( $z = 1.0$  V).

### SFM in Ethanol Prior to the Interaction with Vesicles.

Functional group dominated contrast (CFM)<sup>26,42</sup> was not observed in the CPEO3–mercaptoethanol system. (The same observations were made for patterns of octadecanethiol–mercaptoethanol.) For measurements in ethanol the predicted contrast (friction and pull-off forces, tip–substrate, or vice versa) between functional groups is in the order OH:OH > CH<sub>3</sub>:CH<sub>3</sub> > OH:CH<sub>3</sub>.<sup>26,42</sup> The expected order of pull-off forces was observed for both the COOH tips (OH > CPEO3) and the –CH<sub>3</sub> probes (CPEO3 > OH). Untreated silicon nitride tips showed no significant contrast in pull-off forces. However, friction measurements made using –CH<sub>3</sub> and COOH functionalized tips and unmodified silicon nitride tips in ethanol revealed that the mercaptoethanol part *always* shows *higher* friction than the cholesterol part.

It is evident that the pull-off forces for the –CH<sub>3</sub> probe did not correlate with the observed friction. These observations indicate that the mercaptoethanol part is disordered and therefore gives rise to considerable friction (energy dissipation).<sup>43,44</sup> Thus, to interpret the friction and adhesion images, both the interaction between functional groups (adhesion) as well as structural parameters (contact area and energy dissipation) have to be taken into account.

**SFM in Water Prior to the Interaction with Vesicles.** On the patterned SAMs, prior the interaction with vesicles, the friction observed in water with underivatized tips is *lower* on the mercaptoethanol regions than on the CPEO3 regions. The contrast observed is dominated by hydrophobic forces.<sup>45</sup> The mercaptoethanol-functionalized surface area is solvated to a much higher degree than the hydrophobic CPEO3 part. Therefore, the forces between the tip and the CPEO3 part are higher than on the mercaptoethanol parts. Consistently, the pull-off forces were higher on the CPEO3 part. As the adhesion forces dominate the interaction between tip and surface in this case, the friction forces show the same trend. By using chemically modified (hydrophobic) SFM tips, the contrast in the friction

(42) Noy, A.; Veznev, D. V.; Lieber, C. M. *Annu. Rev. Mater. Sci.* **1997**, 27, 381.

(43) Xiao, X.; Hu, J.; Charych, D. H.; Salmeron, M. *Langmuir* **1996**, 12, 235.

(44) Lio, A.; Charych, D. H.; Salmeron, M. *J. Phys. Chem. B* **1997**, 101, 3800–3805.

(45) Sinniah, S. K.; Steel, A. B.; Miller, C. J.; Reutt-Robey, J. E. *J. Am. Chem. Soc.* **1996**, 118, 8925.

(41) Berger, C. E. H.; van der Werf, K. O.; Kooyman, R. P. H.; de Grooth, B. G.; Greve, J. *Langmuir* **1995**, 11, 4188.

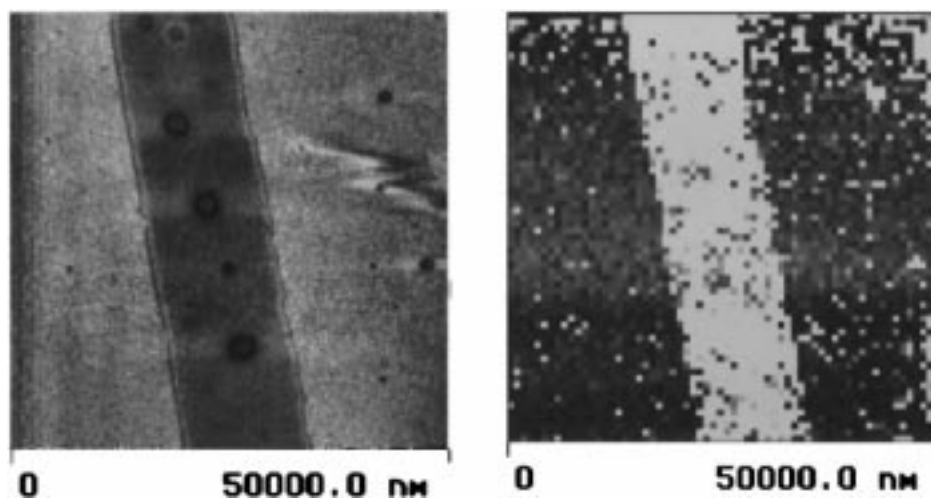


**Figure 3.** Friction force micrograph (left,  $z = 0.2$  V) and adhesion images (right,  $z = 20$  nN) measured with a  $-\text{CH}_3$  modified tip on a patterned SAM prior to interaction with vesicles. In the adhesion image, darker areas correspond to higher adhesion (convention by the SFM producer DI).

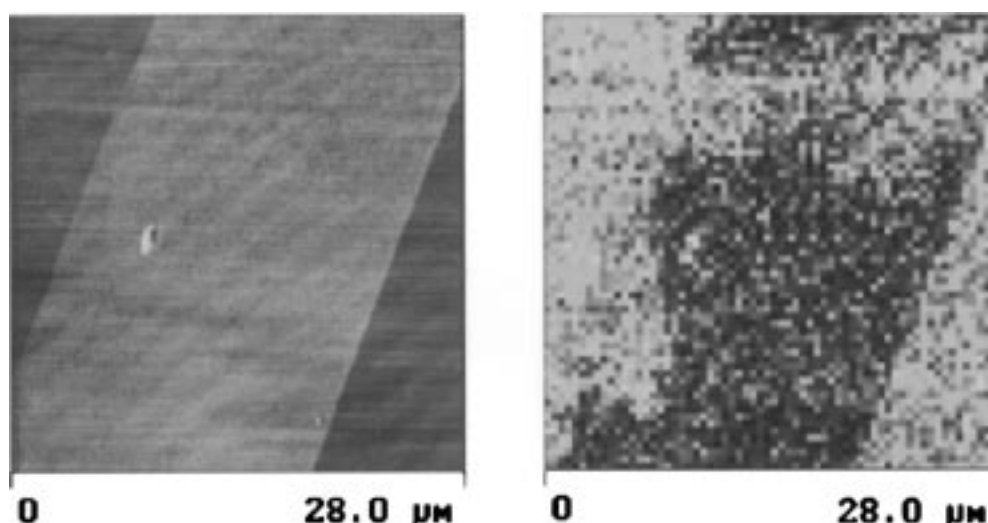


**Figure 4.** Friction force micrograph (left,  $z = 0.4$  V) and adhesion images (right,  $z = 20$  nN) measured with an unmodified tip on a patterned SAM after interaction with vesicles. In the adhesion image, the darker areas correspond to higher adhesion (convention by the SFM producer DI).

and adhesion images of the bare SAMs could be enhanced (Figure 3). The octadecanethiol-modified tips are much more hydrophobic than standard silicon nitride tips. Thus, the hydrophobic forces are strong because *both* tip and CPEO3 surfaces are not solvated.<sup>45</sup>

**SFM in Water after the Interaction with Vesicles.** Following the interaction with vesicles the friction contrast was reversed (Figure 4). Now the mercaptoethanol areas showed *higher* friction. The lateral force on each of the patterns was uniform which is indicative of homogeneous monolayer/bilayer formation on the patterned SAM. The observed contrast cannot be explained by differences in the forces between tip and surface functional groups because the functional groups exposed at the surface are the *same*. However, the mechanical properties of the lipid monolayer on the more rigid CPEO3 part are different from the more fluid lipid bilayer on top of the mercaptoethanol.<sup>36</sup> At a given imaging force, the SFM tip penetrates more into the lipid bilayer, and consequently, the contact area between tip and sample is increased. This results in an increase in friction since (in the absence of wear) the friction force is directly proportional to the contact area ( $F = \tau A$ , where  $F$  denotes the friction force,  $\tau$  the interfacial shear strength, and  $A$  the contact area).<sup>46</sup> The increased contact area is also seen in the adhesion images (Figure 4).

When octadecanethiol-functionalized tips were used, the relative image contrast in both friction and adhesion images remained unchanged as compared to silicon nitride tips. However, the magnitude of the pull-off forces as well as the contrast in the adhesion images was found to be smaller. These observations are consistent with the interpretation of the image contrast (*vide supra*) and the expected interaction between octadecane thiol functionalized tips and hydrophilic surfaces in water.<sup>28,45</sup>

**SPR Kinetics.** The SPR curves obtained for the stamped SAM before and after lipid addition are shown in Figure 5. The increase in the relative intensity of the reflected light, at  $\theta_{\min} - 0.5^\circ$ , during the interaction with vesicles is shown in Figure 6. It is evident from the kinetics data that the adsorption is a two-stage process involving a sharp initial increase in film thickness followed by a longer period during which there is only a small increase in the optical thickness of the film. It should be noted however that the adsorption observed here is much slower than found on hydrophilic surfaces and indicates that the adsorption data are dominated by the adsorption onto the hydrophobic portions of the surface. While stable lipid layers are formed, as evidenced from “flushing” the cells with electrolyte, the optical

(46) Bar, G.; Rubin, S.; Parikh, A. N.; Swanson, B. I.; Zawodzinski, T. A. Jr.; Whangbo, H.-W. *Langmuir* **1997**, *13*, 373–377.

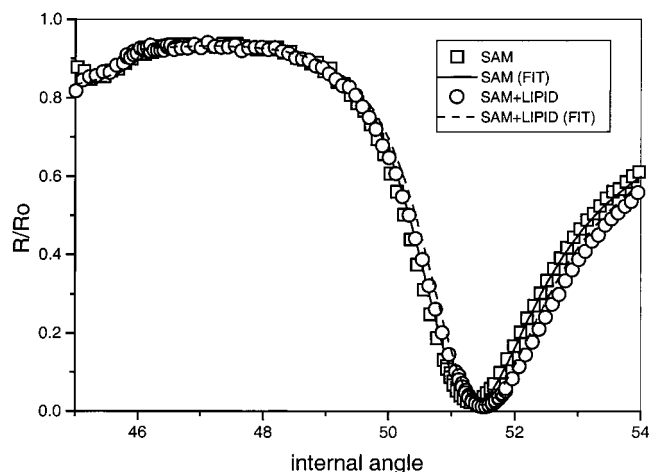


**Figure 5.** Surface plasmon resonance curves obtained before and after vesicle interaction with a micropatterned substrate.

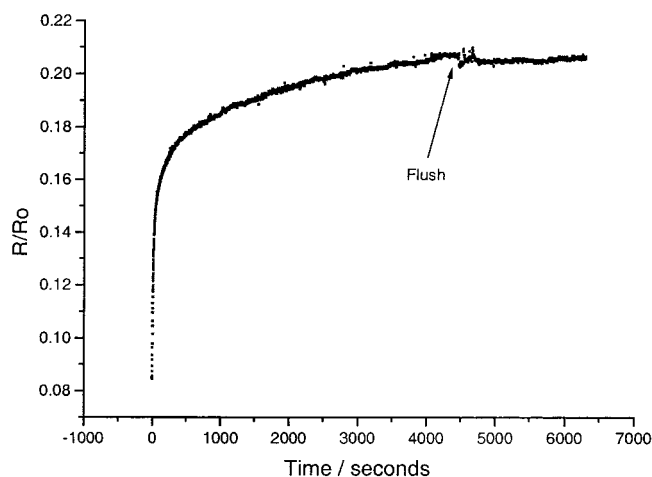


**Figure 6.** Kinetics of lipid adsorption on a micropatterned SAM obtained by monitoring the reflected intensity at a fixed angle,  $\theta_{\min} = 0.5^\circ$ .

thickness of the adsorbed layer is still increasing slowly, suggesting that adsorption process was not completed within the duration of the SPR experiment (2 h). The thickness of the lipid film, determined from fitting the SPR curves before and after lipid adsorption, is approximately  $17 \text{ \AA}$ . This value is within experimental error,  $18 \pm 2 \text{ \AA}$ , of the those obtained in our previous studies of EPC adsorption onto hydrophobic supports and is slightly lower than we would anticipate for a complete lipid monolayer.<sup>13</sup> This suggests either incomplete monolayer formation or that the adsorbed lipid monolayer has different structural properties (i.e., with a different optical density) than lipids within adsorbed bilayers bilayers. Interestingly, we have consistently found that "best-fits" of our lipid monolayer adsorption data are achieved using lipid refractive index values close to 1.46, while for adsorbed lipid bilayers, we find that refractive index values ca. 1.5 produce the "best fits".<sup>13</sup>

**Electrochemical Impedance Measurements. Kinetics.** A detailed account of the derivation of the resistance and capacitance terms from the impedance spectra is given in our previous communication.<sup>21</sup> The kinetics of bilayer formation were measured electrochemically by performing sequential impedance scans, 1 min apart (scan duration is 2 min), for the first 8 scans, then at longer intervals for up to 18 h. The resultant capacitance was plotted as a function of time. The capacitance changes as a result the lipid film forming on the surface, which

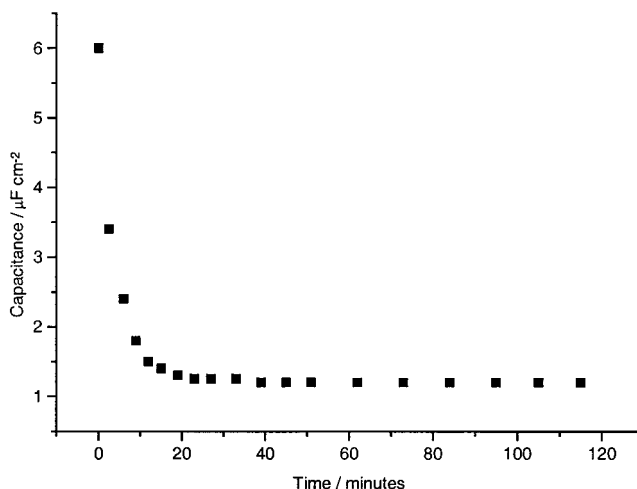


**Figure 7.** Kinetics of lipid adsorption on a micropatterned SAM substrate determined from the change in capacitance of the sample.

behaves electrically like a capacitor dielectric. Since the capacitance of the lipid film is up to a factor of 10 *smaller* than the SAM, it follows that as the film forms the total measured capacitance will be dominated by the capacitance of the lipid film. As a result, monitoring the capacitance change on lipid addition allows the kinetics of lipid film formation to be followed. In addition, the lipid film spans areas in the SAM of high specific capacitance, i.e. areas of mercaptoethanol or bare gold. As such areas are gradually covered by lipid, their contribution to the total capacitance decreases.<sup>21</sup>

Figure 7 shows typical capacitance/time during the interaction of large EPC vesicles with a microcontact printed SAM on gold. It is evident that the greatest changes in the capacitance take place within the first 40 min. Typically, however, the capacitance continues to decrease over the next 18 h to a limiting value of  $0.9 \mu\text{F cm}^{-2}$  in 0.1 M  $\text{BaCl}_2$ .

We note the relative similarity of adsorption kinetics when measured by SPR and impedance: both show a sharp initial adsorption followed by a longer period of reorganization on the surface. In both cases, the greatest change in intensity takes place within the first 10 min and little change in either capacitance or reflected intensity is noted after 60 min.

**Ion Selectivity.** The introduction of ionophores into the lipid bilayer facilitates the detection/passage of specific ions. Two types of ionophore have been used here: one, gramicidin, is a channel-forming peptide, while the other, valinomycin, is an ion transporter. To incorporate valinomycin into the bilayer, the valinomycin was dried down with the lipid prior to dispersion in electrolyte and then dispersed and extruded with the lipid to form vesicles. The initial valinomycin concentration was 0.5 mol % of the total EPC lipid present. The resulting vesicles contain valinomycin, and upon interaction with the surface, a bilayer containing valinomycin is formed. Gramicidin was incorporated into existing bilayers via diffusion from an aqueous suspension in 0.1 M  $\text{BaCl}_2$  following sonication and vortexing. It should be noted that in both experiments we have no knowledge of the final concentration of valinomycin or gramicidin present in the adsorbed lipid layer.

Ion conductance across the resulting bilayer/ionophore structures is dominated by (1) defects in the bilayer and (2) ionophore activity. However, only the ionophore activity will show ion selectivity. Figures 8 and 9 demonstrate the preferential transport of specific ions across a bilayer in the presence of the ionophores.



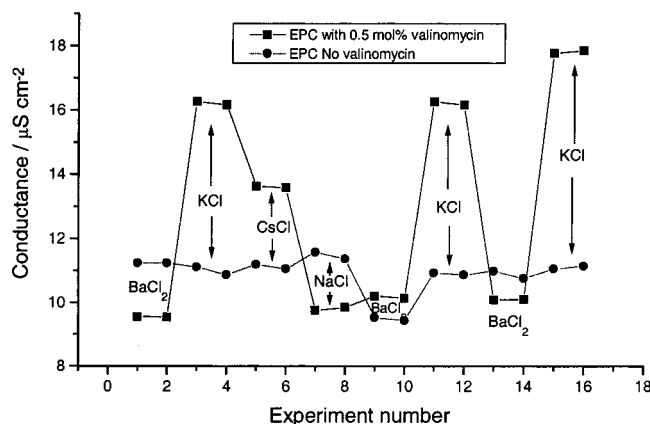


**Figure 8.** Conductance for a lipid layer containing valinomycin in the presence of electrolyte containing different cations (all at 0.1 M).

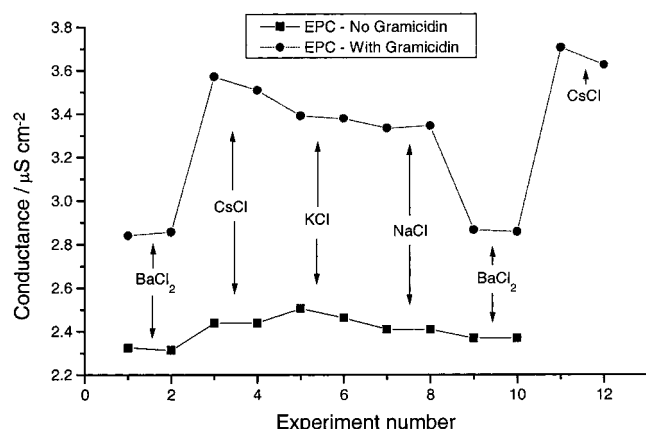


**Figure 9.** Conductance of a lipid layer containing gramicidin in the presence of electrolyte containing different cations (all at 0.1 M).

**Valinomycin.** Valinomycin is an ion carrier ionophore that transports ions across lipid membranes with particular affinity for potassium. The arrangement of carbonyl groups on the six Val residues forms an octahedral cavity that is the optimum size for coordinating the potassium ion.<sup>47</sup> Figure 8 illustrates the ion selectivity of valinomycin incorporated into the lipid vesicles at 0.5 mol %. The increased conductance of potassium can clearly be seen compared with barium, which valinomycin should show no selectivity for. The other ions ( $\text{Cs}^+$  and  $\text{Na}^+$ ) show the expected conductance sequence between the potassium and barium.<sup>48</sup> It is clear from Figure 8 that the preferential conductance of potassium compared to barium is highly reproducible and repeatable. Figure 8 also shows the control experiment on an identical bilayer, without valinomycin, where no selectivity for potassium is observed.

**Gramicidin.** Gramicidin A is a pentadecapeptide with alternating D- and L-amino acids that form a conducting pore through lipid bilayers.<sup>49</sup> The functional pore form exists as a

head-head dimer of  $\beta^{6.3}$  helices.<sup>50</sup> The pore is 4 Å in diameter and shows a selectivity for group 1 cations in proportion to the size of hydrated ions. A typical result from an experiment measuring the conductance of ions through gramicidin ion channels in an EPC the bilayer is given in Figure 9. Here measurements were made on the pure EPC bilayer both before and after adding gramicidin. It is clear that the presence of gramicidin has a somewhat detrimental effect on the overall blocking nature of the bilayer. However, a clear selectivity for cesium is observed, with an overall conductance sequence ( $\text{Cs}^+ > \text{K}^+ > \text{Na}^+ \gg \text{Ba}^{2+}$ ) in agreement with literature measurements of gramicidin conductance in black lipid membranes.<sup>51</sup> Gramicidin is reported to be blocking to barium ions.<sup>49</sup> Once again the changes in conductance were found to be highly reproducible.

It is evident from Figures 8 and 9 that there is a variation in the background conductance levels in the absence of valinomycin or gramicidin. This variation might have a variety of sources, including the roughness of the gold, defects introduced during stamping, or poor lipid coverage. While at present we cannot determine the exact nature of the variation of the background level, we do only observe cation selectivity in the presence of gramicidin and valinomycin.

## Conclusion

This paper demonstrates a new method for attaching lipid bilayers to solid substrates. The combination of microcontact printing and self-assembly of lipid vesicles allows the construction of a tethered biomimetic membrane. We have demonstrated from SFM measurements that, by microcontact printing lipophilic self-assembled monolayers on gold, we can construct a regular array of mercaptoethanol filled "wells", within which lipid bilayers will form. The kinetics of formation of lipid bilayers in these wells have been measured using both surface plasmon resonance and impedance spectroscopies. Importantly, we illustrate that these bilayers retain their biomimetic nature. Our experiments on these systems demonstrates the ion selectivity sequence from fundamental studies of ion channel function.<sup>48–51</sup> The potential for utilizing this new technology for biosensing is exciting. For example, we have demonstrated that potassium can be measured using the valinomycin-containing bilayer, and since the potassium concentration in biological fluids is of clinical interest, the construction of biosensors based on such arrays of supported lipid bilayers will be a logical development of this initial work. Finally, we note that there are some technological issues that need to be addressed before these systems can find application; namely, the variation and magnitude of the background signal need to be minimized.

**Acknowledgment.** We thank the BBSRC for providing financial assistance in support of this work (Grant Reference E06735). S.D.O. acknowledges the EPSRC and DERA for the provision of a CASE studentship.

JA983968S

(47) Neupert-Laves, K.; Dobler, M. *Helv. Chim. Acta* **1975**, 58, 439.

(48) Henderson, P. J. F.; McGivan, J. D.; Chappell, J. B. *Biochem. J.* **1969**, 111, 521.

(49) Woolley, G. A.; Wallace, B. A. *J. Membr. Biol.* **1992**, 129, 109–136.

(50) Urry, D. W.; Goodhall, M. C.; Glickson, J. D.; Mayers, D. F. *Proc. Natl. Acad. Sci. U.S.A.* **1971**, 68, 1907–1911.

(51) Hill, B. *Ionic Channels of Excitable Membranes*, 2nd ed.; Sinauer Associates: Sunderland, MA, 1992; pp 305–312.